Astronomy & Astrophysics manuscript no. Localstructuredipole
May 26, 2014
© ESO 2014

Impact of local structure on the cosmic radio dipole

Matthias Rubart[1]⋆, David Bacon[2] ⋆⋆, Dominik J. Schwarz[1]⋆⋆⋆

[1]Fakultät für Physik, Universität Bielefeld, Postfach 100131, 33501 Bielefeld, Germany
[2]Institute of Cosmology and Gravitation, University of Portsmouth, Burnaby Road, Portsmouth PO1 3FX, United Kingdom

Preprint online version: May 26, 2014

ABSTRACT

We investigate the contribution that a local over- or under-density can have on linear cosmic dipole estimations. We focus here on radio surveys, such as the NRAO VLA Sky Survey (NVSS), and forthcoming surveys such as those with the LOw Frequency ARray (LOFAR), the Australian Square Kilometre Array Pathfinder (ASKAP) and the Square Kilometre Array (SKA). The NVSS has already been used to estimate the cosmic radio dipole; it was shown recently that this radio dipole amplitude is larger than expected from a purely kinematic effect, assuming the velocity inferred from the dipole of the cosmic microwave background. We show here that a significant contribution to this excess could come from a local void or similar structure. In contrast to the kinetic contribution to the radio dipole, the structure dipole depends on the flux threshold of the survey and the wave band, which opens an opportunity to distinguish the two contributions.

Key words. observational cosmology, large scale structure, radio surveys, peculiar motion

arXiv:1402.0376v2 [astro-ph.CO] 23 May 2014

1. Introduction

In recent years, the dipole anisotropy in radio surveys, such as the NVSS catalogue (Condon et al. 1998), has been investigated (e.g. Blake & Wall (2002), Singal (2011), Gibelyou & Huterer (2012), Rubart & Schwarz (2013) and Kothari et al. (2013)). It appears that the cosmic radio dipole has a similar direction to the one found in the Cosmic Microwave Background (CMB), but with a significantly higher amplitude (by a factor of three to four, based on different estimators and surveys (Singal 2011; Rubart & Schwarz 2013)). In this work we investigate one possible effect which can increase the dipole amplitude observed in radio surveys, with respect to the CMB dipole.

There have recently been studies (e.g. Keenan et al. (2013) and Whitbourn & Shanks (2014)) which claim that the local universe (i.e. on scales of 300 Mpc) has an atypically low density of galaxies. If we do live in such a region, what would we expect to see regarding the observed cosmic radio dipole? We are unlikely to be living in the very centre of such a void, so there will be some offset distance between us and the centre of the void, which we call $\boldsymbol{r}_\mathrm{v}$. If we imagine a sphere around the observer (in our case the Local Group), with a radius R_o greater than the void radius R_v, we will expect to see more galaxies in one direction than in the other.

It is likely that the Local Group moves towards the direction where we see more galaxies, due to their gravitational pull. This direction has been determined to be $(l, b) = (276^\circ \pm 3^\circ, 30^\circ \pm 3^\circ)$ (Kogut et al. 1993) in galactic coordinates. The CMB dipole, $(l, b) = (263.99^\circ \pm 0.14^\circ, 48.26^\circ \pm 0.03^\circ)$ from Hinshaw et al. (2009), is caused by the motion of the Sun relative to the CMB, while the radio dipole, $(l, b) = (248^\circ \pm 28^\circ, 46^\circ \pm 19^\circ)$ from Rubart & Schwarz (2013), can be expected to receive contributions from the motion of the Solar System with respect to the CMB (kinetic dipole) and due to the uneven galaxy distribution (structure dipole). Within the current accuracy, the direction of the radio dipole agrees with the CMB direction as well as with the motion of the Local Group with respect to the CMB. Therefore we expect the contribution of a local void to the radio dipole to add up with the velocity dipole, resulting in a larger dipole amplitude in radio surveys.

The local structures considered in this work are not in conflict with the Copernican principle, as they are much smaller than the Hubble scale and thus a fine tuning of the position of the observer with respect to the centre of a void is not required. This is different to scenarios in which huge voids have been invoked to provide an alternative explanation of dark energy (e.g. Celerier (2000), Alnes et al. (2006), Alnes & Amarzguioui (2006)).

In this work, we will investigate this chain of thought in a more quantitative manner. Our model will be discussed in section 2, followed by detailed testing in section 3. In section 4 we will examine the effects of realistic voids on the dipole, and we will present our conclusions in section 5.

2. Model

For simplicity we model the observed universe limited by a radius of R_o and with constant mean number density of sources everywhere (except in the area occupied by the void). Therefore the results of this section can not directly be compared to radio surveys. The more realistic case of a flux limited observation, with certain number counts, is discussed in section 4.

The configuration of our model can be seen in figure 1. We consider a density contrast $\delta(r)$ in a region with radius R_v, which we will call a void (but could be any amount of over- or under-density). We can restrict the calculation to the regions where $\delta(r) \neq 0$, as the contribution of the mean density to the dipole amplitude vanishes due to isotropy.

⋆ matthiasr at physik dot uni-bielefeld dot de
⋆⋆ david dot bacon at port dot ac dot uk
⋆⋆⋆ dschwarz at physik dot uni-bielefeld dot de

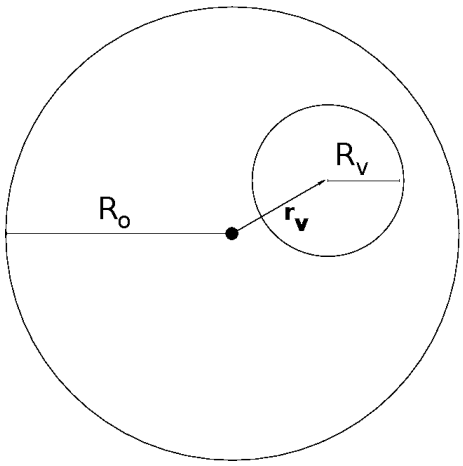

Fig. 1. Configuration of our model of the observed volume-limited universe (radius R_o) with a void of size R_v at distance r_v from the observer.

For the dipole measurement we use the linear estimator introduced by Crawford (2009),

$$\boldsymbol{d} = \frac{1}{N}\sum_{i=1}^{N}\hat{\boldsymbol{r}}_i, \tag{1}$$

where $\hat{\boldsymbol{r}}_i$ is the normalized direction of source i on the sky as seen by an observer in the centre of the observed universe. The fact that this estimator is linear is a big advantage here, since we can sum up the contributions of the background, of voids and of over-densities in an additive way. With a quadratic estimator this would not work out so trivially.

In order to simplify the integration, we pick a coordinate system centered on the void. The expectation of the observed dipole from the void, measured with the estimator (1), will be

$$\langle\boldsymbol{d}\rangle = \bar{\alpha}\int_0^{2\pi}\mathrm{d}\varphi\int_{-1}^{1}\mathrm{d}\cos\vartheta\int_0^{R_\mathrm{v}}\mathrm{d}r\,\delta(r)r^2\frac{\boldsymbol{r}-\boldsymbol{r}_\mathrm{v}}{|\boldsymbol{r}-\boldsymbol{r}_\mathrm{v}|}\,. \tag{2}$$

Here we have a normalization factor $\bar{\alpha}$.

As a first case, we assume a constant density contrast δ in the void, and an offset $\boldsymbol{r}_\mathrm{v}$ of the void in direction $\hat{\boldsymbol{z}}$,

$$\langle d_z\rangle = \bar{\alpha}\,\delta\int_0^{2\pi}\mathrm{d}\varphi\int_{-1}^{1}\mathrm{d}\cos\vartheta\int_0^{R_\mathrm{v}}\mathrm{d}r\,r^2\frac{r\cos\vartheta-r_\mathrm{v}}{\sqrt{r^2-2\cos\vartheta r r_\mathrm{v}+r_\mathrm{v}^2}}. \tag{3}$$

This leads to

$$\langle\boldsymbol{d}\rangle = \frac{4\pi}{3}\bar{\alpha}\,\hat{\boldsymbol{r}}_\mathrm{v}\,\delta\,R_\mathrm{v}^3[\Theta(R_\mathrm{v}-r_\mathrm{v})(\frac{r_\mathrm{v}}{R_\mathrm{v}}-\frac{1}{5}\frac{r_\mathrm{v}^3}{R_\mathrm{v}^3}) +\Theta(r_\mathrm{v}-R_\mathrm{v})(1-\frac{1}{5}\frac{R_\mathrm{v}^2}{r_\mathrm{v}^2})]\,, \tag{4}$$

where Θ is the Heaviside function. This formula provides the dipole contribution of a top hat over- or underdensity for an observer inside or outside the void.

Our aim is to investigate void regions with arbitrary density contrast profiles $\delta(r)$. In order to do so, we can heuristically linearly add up a large number N of these voids to get to a smooth distribution $\delta(r)$.

The normalization factor $\bar{\alpha}$ in (4) can be found by the requirement that the integration over a sphere (with radius R_o bigger than the void size R_v) should equal unity,

$$1 = \bar{\alpha}4\pi\left(\int_{R_\mathrm{v}}^{R_\mathrm{o}}\mathrm{d}r\,r^2+\int_0^{R_\mathrm{v}}\mathrm{d}r\,r^2(1+\delta(r))\right), \tag{5}$$

leading to

$$\bar{\alpha} = \frac{3}{4\pi}\frac{1}{R_\mathrm{o}^3+3\int_0^{R_\mathrm{v}}\mathrm{d}r\,r^2\delta(r)}\,. \tag{6}$$

We can see that the prefactor $\frac{3}{4\pi}$ cancels in (4). For convenience we introduce $\alpha = \frac{4\pi}{3}\bar{\alpha}$ for all following formulae.

Let us consider the limit of a distant void $r_\mathrm{v} \gg R_\mathrm{v}$. Then we obtain

$$\lim_{r_\mathrm{v}\gg R_\mathrm{v}}\langle d_z\rangle = \delta\frac{R_\mathrm{v}^3}{R_\mathrm{o}^3}\,. \tag{7}$$

So the dipole amplitude due to a void depends on the density contrast of the void and on the fraction of volume it occupies in the observed universe.

For a realistic case of a flux limited observation of the universe, we need to generalise this formula to

$$\lim_{r_\mathrm{v}\gg R_\mathrm{v}}\langle d_z\rangle \approx \delta\frac{\tilde{N}_\mathrm{v}}{N_\mathrm{o}}\,. \tag{8}$$

Here N_o is the number of sources in the observed universe and $\tilde{N}_\mathrm{v}$ is the number of sources we expect to see in the area occupied by the void, if it had the same mean number density as the rest of the universe. This number does depend on the flux limit, on the functional shape of the number counts and on the distance and size of the void.

2.1. Observers outside the void

Now we want to derive the expectation value of the dipole amplitude from voids with a density contrast $\delta(r)$, which is not constant. To do so, we will add up N concentric voids, resulting in a structure of N concentric shells, each with constant density contrast $\delta_i, i = 1,\ldots,N$. The shells are ordered by their radius, starting at the shell with the biggest radius (shell number 1).

We only look at the absolute value of $\langle\boldsymbol{d}\rangle$, since for symmetry reasons, the direction of this expectation value will always be $\hat{\boldsymbol{r}}_\mathrm{v}$. First we look at N voids as observed from outside the voids, thus $r_\mathrm{v} > R_\mathrm{v}$. The second term in (4) will give N terms, which can be written as

$$\begin{aligned}|d_z| \;=\; \alpha\Big[&\delta_1R_1^3(1-\frac{1}{5}\frac{R_1^2}{r_\mathrm{v}^2})+(\delta_2-\delta_1)R_2^3(1-\frac{1}{5}\frac{R_2^2}{r_\mathrm{v}^2})+\\ &\ldots+(\delta_N-\delta_{N-1})R_N^3(1-\frac{1}{5}\frac{R_N^3}{r_\mathrm{v}^2})\Big]\,.\end{aligned} \tag{9}$$

From this we obtain

$$\begin{aligned}|d_z| \;=\; &\alpha\delta_NR_N^3(1-\frac{1}{5}\frac{R_N^2}{r_\mathrm{v}^2})+\\ &\alpha\sum_{i=1}^{N-1}\delta_i(R_i^3-\frac{1}{5}\frac{R_i^5}{r_\mathrm{v}^2}-R_{i+1}^3+\frac{1}{5}\frac{R_{i+1}^5}{r_\mathrm{v}^2})\,.\end{aligned} \tag{10}$$

Now we take the difference in size between consecutive shells to be infinitesimally small, meaning $R_{i+1} = R_i - \epsilon$. Without loss of

generality, we can put $R_1 = r_\mathrm{v}$ and therefore place the observer on the edge of the biggest void shell (if $r_\mathrm{v} > R_\mathrm{v}$ then $\delta(r)|_{r>R_\mathrm{v}} = 0$). The innermost void shell will have a vanishing radius and so $R_N = 0$. This leads to

$$|d_z| = \alpha \sum_{i=1}^{N-1} \delta_i (3R_i^2 \epsilon - \frac{R_i^4 \epsilon}{r_\mathrm{v}^2}) \,, \tag{11}$$

which can be written in the form of an integral

$$|d_z| = \alpha \int_0^{r_\mathrm{v}} \mathrm{d}\mathrm{r}\, \mathrm{r}^2 \delta(\mathrm{r}) \left(3 - \frac{\mathrm{r}^2}{\mathrm{r}_\mathrm{v}^2}\right). \tag{12}$$

This is the equation we have been seeking for the dipole observed by an observer outside the void.

2.2. Observers inside the void

Now we examine the case of N void shells, each of constant density, with $r_\mathrm{v} \leq R_\mathrm{v}$; the observer is inside the void. We have

$$\begin{aligned} |d_z| \;=\; \alpha \Big[& \delta_1 (R_1^2 r_\mathrm{v} - \frac{1}{5} r_\mathrm{v}^3) + (\delta_2 - \delta_1)(R_2^2 r_\mathrm{v} - \frac{1}{5} r_\mathrm{v}^3) + \\ & \ldots + (\delta_N - \delta_{N-1})(R_N^2 r_\mathrm{v} - \frac{1}{5} r_\mathrm{v}^3) \Big]. \end{aligned} \tag{13}$$

This can be rewritten as

$$|d_z| = \alpha \delta_N (R_N^2 r_\mathrm{v} - \frac{1}{5} r_\mathrm{v}^3) + \alpha \sum_{i=1}^{N-1} \delta_i (R_i^2 r_\mathrm{v} - R_{i+1}^2 r_\mathrm{v}) \,. \tag{14}$$

Again we make the difference in size between consecutive void shells infinitesimally small, meaning $R_{i+1} = R_i - \epsilon$. The shell with the smallest radius that still includes the observer ($r_\mathrm{v} \leq R_\mathrm{v}$), will have $R_{vN} = r_\mathrm{v}$ and $\delta_N = \delta(r_\mathrm{v})$. The void shell with the biggest radius will have $R_1 = R_\mathrm{v}$. This leads to

$$|d_z| = \frac{4}{5} \alpha \delta(r_\mathrm{v}) r_\mathrm{v}^3 - 2\alpha r_\mathrm{v} \sum_{i=1}^{N-1} \delta_i R_{vi} \epsilon, \tag{15}$$

which can be written as an integral

$$|d_z| = \frac{4}{5} \alpha r_\mathrm{v}^3 \delta(r_\mathrm{v}) + 2\alpha r_\mathrm{v} \int_{r_\mathrm{v}}^{R_\mathrm{v}} \mathrm{d}r\, r \delta(r). \tag{16}$$

This is the form we have been seeking for the dipole observed when the observer is inside a void.

2.3. Structure dipole amplitude

When combining the results for an observer inside a void (section 2.2) and those for an observer outside the void (section 2.1), we need to be careful. The void shell at the position of the observer r_v and density contrast $\delta(r_\mathrm{v})$ has been counted in both cases. The formula for an observer outside the void (12) gives $\frac{4}{5}\alpha\delta(r_\mathrm{v})r_\mathrm{v}^3$, which is the same result we find for the observer inside the void (16) with $\delta(r)|_{r<R_\mathrm{v}} = \delta(r_\mathrm{v})$. Therefore we need to subtract this term once when combining both cases. We obtain

$$\begin{aligned} \langle \boldsymbol{d} \rangle \;=\; & \alpha \hat{\boldsymbol{r}}_\mathrm{v} \int_0^{\min(r_\mathrm{v}, R_\mathrm{v})} \mathrm{d}\mathrm{r}\, \mathrm{r}^2 \delta(\mathrm{r}) (3 - \frac{\mathrm{r}^2}{\mathrm{r}_\mathrm{v}^2}) + \\ & \alpha \hat{\boldsymbol{r}}_\mathbf{v} \Theta(R_\mathrm{v} - r_\mathrm{v})\, 2 r_\mathrm{v} \int_{r_\mathrm{v}}^{R_\mathrm{v}} \mathrm{d}r\, r \delta(r). \end{aligned} \tag{17}$$

The upper boundary of the first integral is now the minimum of r_v and R_v, since in general it is not guaranteed that $r_\mathrm{v} < R_\mathrm{v}$.

3. Testing

We test our mathematical model with the help of computer simulations. The focus of the first subsection below is to verify the dependence of a dipole contribution on the three void parameters R_v, r_v and δ. Next we allow for a varying density contrast δ with respect to r. Up to this point, we assume a volume limited observation. The flux limited case, including realistic number counts, is discussed in section 4, where we incorporate a radio sky simulation from Wilman et al. (2008).

3.1. Structures of constant density contrast

Let us first look at constant density contrasts $\delta(r) = \delta$ inside the void area. In order to test our calculations, we construct a simple simulation. We draw a random point (with the random number generator Mersenne Twister) inside a three dimensional sphere of radius R_o, which we set to $R_\mathrm{o} = 1$ (which fixes the physical scale). The points inside this sphere are uniformly distributed.

The next step depends on whether we have an underdensity ($\delta < 0$) or an overdensity ($\delta > 0$) of radius R_v. In the first case, we keep all points which are outside the void (this represents the average density of objects, i.e. $\delta = 0$). For each point inside the void, we draw a random number between 0 and 1. If this number is bigger than $\delta + 1$ we drop this point and turn to the next one. If, on the other hand, it is smaller than $\delta + 1$, we keep it and proceed to a new point (this algorithm is simply a Monte Carlo sampling between $\delta = -1$ and $\delta = 0$).

For the case $\delta > 0$, we keep all drawn points inside the overdensity, and draw random numbers ($0 \rightarrow 1$) for points outside the overdensity. Now we drop the point only if the random number is larger than $1/(1 + \delta)$. So we create a map with the desired densities inside and outside the over-/underdense region.

In this way we will draw N points in total, which will be used to measure $\boldsymbol{d}$ via (1). Due to the fact that we can only use finite values of N, our simulation will always have a certain amount of shot noise, whereas our calculations in Section 2 neglected noise. In Rubart & Schwarz (2013) the influence of this shot noise on the expectation value of a linear estimator is discussed. We compare the average outcome of several simulations with

$$\tilde{d} := \sqrt{\langle \boldsymbol{d} \rangle^2 + (0.92/\sqrt{N})^2} \,, \tag{18}$$

where the second term inside the square root comes from the shot noise contribution. For $\langle \boldsymbol{d} \rangle$ we can use the results discussed in section 2, depending on the case we are simulating.

In table (1) we see a comparison between our analytic expectation and the simulated results, for cases where the observer is inside the void. In order to quantify the performance of the theory we estimate the error by $2|(\tilde{d} - d_s)/(\tilde{d} + d_s)|$. We see in table (1) that this error drops as the dipole values increase. This is due to the fact that in those cases the uncertainties due to shot noise are less important. For the case of $r_\mathrm{v} = 0.1$, $R_\mathrm{v} = 0.2$ and $\delta = -0.5$ we see an unusually high error. We repeated this configuration with 20 extra simulations and found an averaged value of $d_s = 0.215 \times 10^{-2}$, which is very close to $\tilde{d}$; so we are confident that this relatively large disagreement arose by chance. In all other cases we see a good agreement between the calculated values and the simulated ones. If the dipole is large, the agreement becomes remarkably good. These results confirm the calculated expectation values of the dipole for voids with $r_\mathrm{v} \leq R_\mathrm{v}$ and constant density contrast δ.

In table (2) we present the comparison for cases with $r_\mathrm{v} \geq R_\mathrm{v}$. Again we can see that the difference between calculation and

r_v	R_v	δ	$\tilde{d}$ (10^{-2})	d_s (10^{-2})	error %
0.1	0.1	-1	0.12	0.13	8,7
0.1	0.2	-1	0.39	0.41	2,8
0.2	0.3	-1	1.69	1.71	1,3
0.2	0.4	-1	3.25	3.28	0,9
0.4	0.4	-1	5.47	5.47	0,0
0.1	0.1	-0.5	0.10	0.11	10,1
0.1	0.2	-0.5	0.21	0.17	20,2
0.2	0.3	-0.5	0.84	0.84	0,2
0.2	0.4	-0.5	1.57	1.54	2,1
0.4	0.4	-0.5	2.65	2.68	1,3
0.1	0.1	1	0.12	0.13	5,7
0.1	0.2	2	0.75	0.76	1,4
0.2	0.3	4	5.92	5.89	0,5
0.2	0.4	5	11.52	11.50	0,1
0.4	0.4	7	24.75	24.70	0,2

Table 1. Comparison of analytic model and simulation for an observer inside a local spherical structure ($r_v < R_v$) with constant density contrast δ. The analytically calculated dipole is denoted by $\tilde{d}$. Each simulated dipole amplitude d_s is an average of 10 simulations with $N = 10^6$ sources each; the error is defined as $2|(\tilde{d} - d_s)/(\tilde{d} + d_s)|$.

r_v	R_v	δ	$\tilde{d}$ (10^{-2})	d_s (10^{-2})	error %
0.1	0.1	-1	0.12	0.10	18.7
0.2	0.1	-1	0.13	0.13	3.3
0.3	0.2	-1	0.74	0.73	1.7
0.4	0.2	-1	0.77	0.77	0.9
0.4	0.4	-1	5.47	5.46	0.2
0.1	0.1	-0.5	0.10	0.11	7.4
0.2	0.1	-0.5	0.10	0.09	12.9
0.3	0.2	-0.5	0.38	0.40	5.8
0.4	0.2	-0.5	0.39	0.36	8.4
0.4	0.4	-0.5	2.65	2.65	0.1
0.1	0.1	1	0.12	0.12	3.2
0.2	0.1	2	0.21	0.21	2.3
0.3	0.2	4	2.83	2.81	0.6
0.4	0.2	5	3.66	3.66	0.1
0.4	0.4	7	24.75	24.70	0.2

Table 2. As table 1, but for observers sitting outside the spherical structure.

simulation is quite small, and decreases as the dipole amplitude increases.

The simulated dipole amplitude can be plotted as a function of either r_v, R_v or δ. We present examples of simulations in figures 2, 3 and 4, where we have fitted functions of the form (4) making use of the normalization factor (6) and including a shot noise contribution (18).

In all cases the fitted curve follows the simulated dipole amplitudes very well. The first case shows the dipole amplitude as a function of the density contrast δ; we see that the dependence on δ is approximately linear. Here we used a void of size $R_v = 0.4$ and an offset distance of $r_v = 0.2$; we expect from our theoretical model fit parameters of $\langle a \rangle = 0.0305$, $\langle b \rangle = 0.064$ and $\langle c \rangle = 0.92 \times 10^{-3}$. The values of our fit of $f(\delta)$ give us the parameters $a = 0.0303 \pm 0.0002$, $b = 0.066 \pm 0.005$ and $c = (0.92 \pm 0.05) \times 10^{-3}$, which are in excellent agreement.

For figure 3 we used 10^6 sources, a density contrast of $\delta = -1$ and a void radius of $R_v = 0.3$; we expect $\langle a \rangle = 0.0925$, $\langle b \rangle = 0.206$ and $\langle c \rangle = 0.92 \times 10^{-3}$. The values of our fit of $g(r_v)$ give us the parameters $a = 0.0924 \pm 0.0002$, $b = 0.205 \pm 0.003$ and $c = (0.92 \pm 0.04) \times 10^{-3}$. Again, this is in very good agreement with our prediction. We can observe that the dipole increases strongly with the offset distance r_v. On the edge of the void, the increase becomes more modest.

The graph in figure 4 shows the behaviour of the dipole amplitude as a function of the void size R_v. Here we used a density contrast of $\delta = -0.25$ and an offset distance of $r_v = 0.2$; we expect $\langle a \rangle = 0.2$, $\langle b \rangle = 0.25$ and $\langle c \rangle = 0.92 \times 10^{-3}$. The values of our fit of $h(R_v)$ give us the parameters $a = 0.205 \pm 0.006$, $b = 0.244 \pm 0.006$ and $c = (0.91 \pm 0.07) \times 10^{-3}$. We see that the parameters are in very good agreement with our prediction.

We conclude from this section that formula (4) combined with (18) is in very good agreement with our simulations.

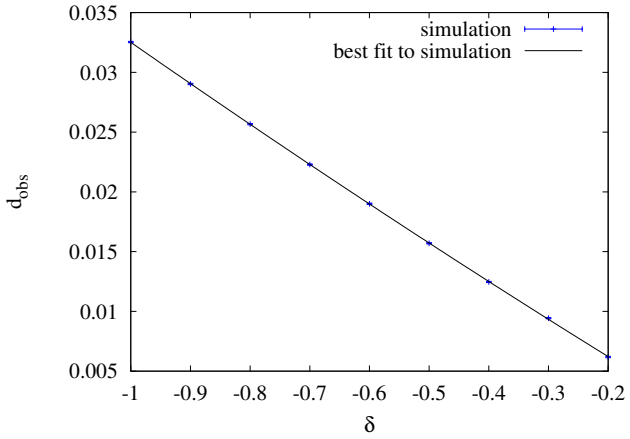

Fig. 2. Simulated dipole amplitudes. The graph is for a void with $R_v = 0.4$ and $r_v = 0.2$ for different values of δ, while the curve is the best fit. Each data point is the mean value of the dipole amplitude from 100 simulations with 10^6 sources each. The error bars represent the empirical variance of these simulations. For the fit a function $f(\delta) = \sqrt{\left(\delta \frac{a}{1+b\delta}\right)^2 + c^2}$ was used.

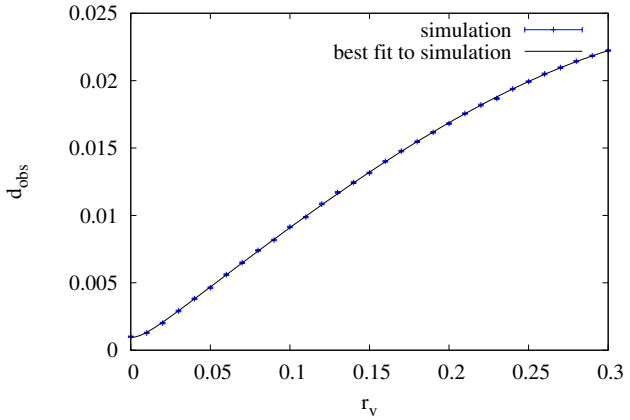

Fig. 3. Simulated dipole amplitudes. The graph is for a void with $R_v = 0.3$ and $\delta = -1$ for different values of r_v. Each data point is the mean value of the dipole amplitude from 100 simulations with 10^6 sources each, while the curve is the best fit. The error bars represent the empirical variance of these simulations. For the fit, a function $g(r_v) = \sqrt{(a\, r_v - b\, r_v^3)^2 + c^2}$ was used.

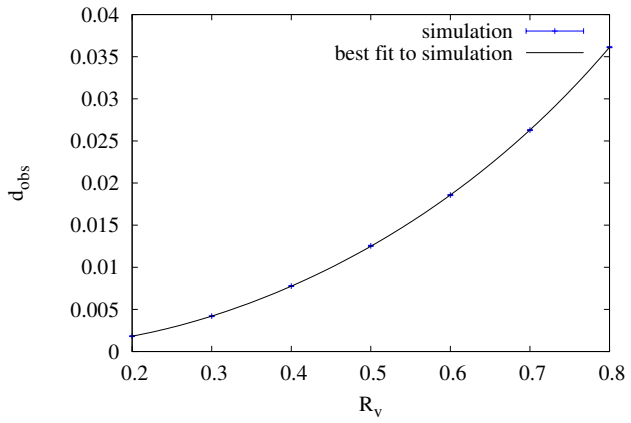

Fig. 4. Simulated dipole amplitudes. The graph is for a void with $r_\mathrm{v} = 0.2$ and $\delta = -0.25$ for different values of R_v. Each data point is the mean value of the dipole amplitude from 100 simulations with 10^6 sources each, while the curve is the best fit. The error bars represent the empirical variance of these simulations. For the fit, a function $h(R_\mathrm{v}) = \sqrt{\left(b\frac{a\,R_\mathrm{v}^2 - 0.2a^3}{1+b\,R_\mathrm{v}^3}\right)^2 + c^2}$ was used.

r_v	R_v	p	$\tilde{d}$ (10^{-2})	d_s (10^{-2})	error %
0.2	0.4	1	0.96	0.96	0.2
0.3	0.5	1	2.16	2.18	0.7
0.2	0.4	2	1.49	1.51	1.4
0.3	0.5	2	3.42	3.44	0.4
0.2	0.4	3	1.82	1.83	0.2
0.3	0.5	3	4.24	4.25	0.2

Table 3. Comparison for cases with offset distance r_v smaller than void radius R_v. The density contrast is of the form $\delta(r) = \frac{r^p}{R_\mathrm{v}^p} - 1$ and the calculated dipole is $\tilde{d}$. Each simulated dipole amplitude d_s is an average of 10 simulations with $N = 10^6$ sources each; the error is defined as $2|\frac{\tilde{d}-d_s}{\tilde{d}+d_s}|$.

3.2. Arbitrary void profile

Now we would like to test whether formula (17) is also verified by our simulations. We consider density contrasts of the form $\delta(r) = \frac{r^p}{R_\mathrm{v}^p} - 1$ for r inside the void and $\delta(r) = 0$ outside. In all such cases the density contrast has the boundary values $\delta(0) = -1$ and $\delta(R_\mathrm{v}) = 0$. In such cases the integrals in (17) can be solved analytically. Results will be put into (18) in order to get $\tilde{d}$.

The simulation is similar to the one described in section 3.1. We choose a random number for points inside the void. This time a point (with distance r from the void centre) is discarded if the random number is greater than r^p/R_v^p.

In table (3) we see the comparison of our calculated dipole expectation with the simulation results for cases $r_\mathrm{v} < R_\mathrm{v}$, and in table (4) for cases with $R_\mathrm{v} > r_\mathrm{v}$. Again we can observe the tendency to find improved agreement with the analytic model when the dipole amplitude is larger. In fact even for small dipole values we see a good agreement between the simulation and our calculation. Therefore we are satisfied that equation (17) is confirmed by our simulations.

r_v	R_v	p	$\tilde{d}$ (10^{-2})	d_s (10^{-2})	error %
0.4	0.2	1	0.21	0.21	1.9
0.5	0.3	1	0.65	0.69	4.7
0.4	0.2	2	0.32	0.31	2.8
0.5	0.3	2	1.04	1.05	1.0
0.4	0.2	3	0.40	0.42	5.1
0.5	0.3	3	1.30	1.30	0.0

Table 4. Comparison for cases with offset distance r_v larger than void radius R_v. The density contrast is of the form $\delta(r) = \frac{r^p}{R_\mathrm{v}^p} - 1$ and the calculated dipole is $\tilde{d}$. Each simulated dipole amplitude d_s is an average of 10 simulations with $N = 10^6$ sources each; the error is defined as $2|\frac{\tilde{d}-d_s}{\tilde{d}+d_s}|$.

4. Missing dipole contribution

Now we investigate the contribution which realistic void models can have on the observed radio dipole. Therefore we no longer assume a volume limited observation, but a flux limited one.

In Rubart & Schwarz (2013), a dipole amplitude $d_\mathrm{radio} = (1.8 \pm 0.6) \times 10^{-2}$ in the NVSS catalogue was reported, which is significantly above the prediction inferred from CMB measurements (Hinshaw et al. 2009) of $d_\mathrm{cmb} = (0.48 \pm 0.04) \times 10^{-2}$. Therefore we can infer a missing dipole contribution

$$\mathbf{\Delta\tilde{d}} = \mathbf{\tilde{d}}_\mathrm{radio} - \mathbf{d}_\mathrm{cmb} = (1.3 \pm 0.6) \times 10^{-2}, \tag{19}$$

where the tilde indicates that the dipole amplitudes include correction factors, which are also be applied to the void dipole estimations below.

We would like to investigate whether it is possible to get a dipole contribution of this magnitude from a void model in which we are off-centre. We examine a void of the type described by Keenan et al. (2013). They report an observed void with a density contrast of about $-\frac{1}{3}$ up to redshifts of about $z = 0.07$. The influence of smaller voids, compared to Keenan et al. (2013), on the clustering dipole, was discussed e.g. by Bilicki & Chodorowski (2010).

Since we want to compare the void dipole d_void with the one derived from the NVSS catalogue, we cannot assume a constant density outside the void. The NVSS itself does not contain information about the distance of individual objects. In order to have a realistic redshift distribution, we used the semi-empirical S^3 simulation from Wilman et al. (2008) with an area of 400 square degrees. From this we obtained a catalogue of approximately 2800 radio sources with flux densities above 25 mJy at 1.4 GHz (the limit Rubart & Schwarz (2013) used for obtaining d_radio). This is now a flux limited observation, in contrast to the volume limited model in the previous section.

Now we modify our void simulation in the following way. Each data point will have a randomly chosen direction on the sky and a redshift distance chosen from the S^3 catalogue. Inside the void we will reduce the density of points in the way described in section 3.1. So we are left with number counts outside the void, which are close to what is actually observed in the mean, and some density contrast $\delta(r)$ inside the void.

We would like to estimate the maximal contribution of such a void to the measured dipole amplitude. Therefore we choose $r_\mathrm{v} = R_\mathrm{v}$, since this will give the biggest dipole amplitude for a void which includes the observer. As we consider r_v to be much less than the Hubble distance R_H, we can use the linear Hubble law to relate distances and redshift. The shot noise in this simulation should be suppressed, since we only want to know the

pure contribution from the void (any possible shot noise is already taken into account by the error bars of $d_{\rm radio}$). So we choose the following parameters for our simulation, which uses the redshift information to infer the distance parameters: $R_{\rm v} = 0.07R_{\rm H}$, $\delta = -1/3$ and $N = 10^7$. We carried out 50 runs of our simulation, and the average dipole we obtained is

$$d_{\rm void} = (0.0918 \pm 0.0023) \times 10^{-2}. \quad (20)$$

For $r_{\rm v} = 0.06R_{\rm H} < R_{\rm v}$ we obtained $d_{\rm void} = (0.0839 \pm 0.0026) \times 10^{-2}$. Lower values of $r_{\rm v}$ lead to lower dipole amplitudes.

Due to masking effects (incomplete sky coverage and galactic foreground) the dipole amplitude in Rubart & Schwarz (2013) was multiplied by $3/k$, where k was evaluated to be 1.34 for this case. In order to compare both dipole amplitudes, we also need to multiply $d_{\rm void}$ by this number,

$$\tilde{d}_{\rm void} = \frac{3}{k} d_{\rm void} = (0.21 \pm 0.01) \times 10^{-2}. \quad (21)$$

If we compare this $\tilde{d}_{\rm void}$ to the missing dipole Δd we can see that such a void can have a significant contribution to the observed radio dipole. When we consider the lower bound of $d_{\rm radio}$ we see that $\tilde{d}_{\rm void}$ could explain up to about a third of the missing radio dipole.

If we would like to explain the missing dipole contribution only by one void, this would need to be bigger and have a larger density contrast. One possible combination of void parameters would be $R_{\rm v} = r_{\rm v} = 0.11R_{\rm H}$ and $\delta = -0.6$. For this we found, with 50 simulations, an average dipole (including masking corrections, described above) of

$$\tilde{d}_{\rm void} = \frac{3}{k} d_{\rm void} = (0.72 \pm 0.01) \times 10^{-2}. \quad (22)$$

A similar result, $d = (0.69 \pm 0.01) \times 10^{-2}$, is obtained with the parameters $R_{\rm v} = r_{\rm v} = 0.15R_{\rm H}$ and $\delta = -1/3$. These void models are not particularly extreme. Another possibility would be to have a combination of different under- and over-densities, such as e.g. superclusters. The dipole of these different structures could add up to result in an amplitude which could potentially explain the whole missing dipole contribution.

4.1. Flux and frequency dependence

So far we only used the S^3 simulation with a lower flux density limit of 25 mJy. For future radio surveys we hope to be able to estimate the radio dipole with more sources and therefore we will need to apply a lower flux density limit. The effect of a change in this flux density limit for the dipole contribution of a void is not trivially estimated. On the one hand, a lower flux density limit means that we can see more distant sources then previously. This means that local structure becomes less important. On the other hand, a lower flux density limit will also lead to the detection of nearby galaxies, which have a low radio brightness. For those galaxies the void structure is important and we could expect an increase in the measured dipole amplitude. Both effects will vary in strength at different flux density ranges.

In order to estimate these effects, we again used the S^3 simulation from Wilman et al. (2008). We considered the two frequencies of 1.4 GHz (e.g. NVSS or a planned survey with ASKAP[1]) and 151 MHz (e.g. LOFAR[2]). A continuum survey

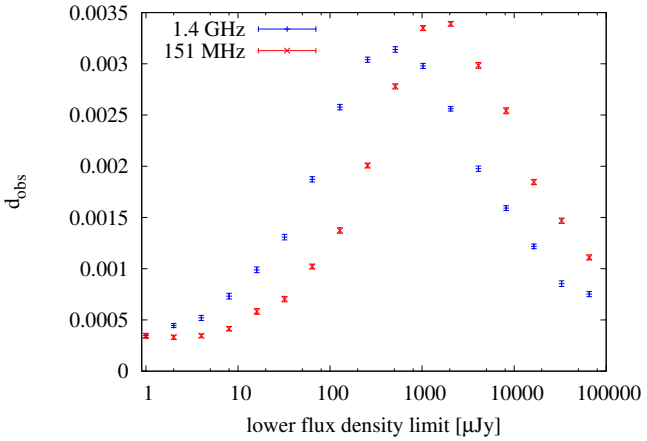

Fig. 5. Simulated dipole amplitudes for different flux limits. Each point is the average of 50 simulations with 10^7 sources each. The void used here has the parameters $R_{\rm v} = r_{\rm v} = 0.07R_{\rm H}$ and $\delta = -1/3$. The error bars represent the empirical variance of these simulations.

with the SKA[3] will be likely to be collected at a frequency between these (e.g. 600 MHz). Again we used the void parameters from Keenan et al. (2013). This time we applied different flux density limits to see the dependence of the observed dipole amplitudes on the flux density limit.

In figure 5 we see that the dependence of the measured dipole amplitudes from the flux density limit is quite complex. Notice that the flux limits shown cover almost five orders of magnitude. For flux density limits below 10 mJy, the dipole amplitudes increase very strongly until a maximum is reached around 1 mJy. The contribution of a local void for the dipole in a survey with a flux density limit of 1 mJy could be about three times as strong as it is for a limit of 25 mJy. This means that the effect of voids will become more important in future radio surveys. In principle it is possible to disentangle the kinetic dipole contribution from the structure dipole, since the kinetic dipole amplitude does not depend on the flux density limit (the shot noise does, but this will be taken into account by the error bars).

We can see that the general behaviour for both frequencies is the same. The main difference is in the position of the peak in the dipole amplitude. This comes from the fact that different radio source populations show up at different flux density limits for different frequencies. Due to this effect it seems possible to analyze the structure component of the radio dipole by using different frequencies and flux density limits. A kind of tomography of the local universe would be a possible application. Radio telescopes like LOFAR, ASKAP or SKA will be ideal to create the necessary radio catalogues at different frequencies for this purpose.

4.2. Line of sight dependence

It was shown by Singal (2011) that the amplitude of a linear dipole estimator (using the NVSS survey), for different areas of the sky, varies like $\cos(\theta)$, where θ is the angle measured between the line of sight and the dipole direction. This analysis is in agreement with the assumption that the radio dipole is dominated by a kinetic contribution.

[1] www.atnf.csiro.au/projects/askap/
[2] www.lofar.org
[3] www.skatelescope.org

We now discuss whether a radio dipole which is partly due to a contribution from a local void, would be in conflict with this observed behaviour or not. Therefore we investigate how the dipole amplitude from a void varies with respect to the angle θ (for simplicity we assume a constant density contrast inside the void here). Any prefactors, which do not depend on θ, are not relevant here.

The effect of a void-like structure on the dipole amplitude is proportional to the length of the line of sight inside the void. If we are inside the void, we need to add the forward and backward contribution, since a dipole estimator also picks up both parts. In order to find this length, we use the equation of a circle (radius R_v) with an offset of r_v in the x-direction

$$(x - r_\mathrm{v})^2 + y^2 = R_\mathrm{v}^2 \,. \tag{23}$$

Using polar coordinates l, θ with $x = l\cos\theta, y = l\sin\theta$ we can transform this to

$$\frac{l}{R_\mathrm{v}} = \frac{r_\mathrm{v}}{R_\mathrm{v}}\cos(\theta) \pm \sqrt{\frac{r_\mathrm{v}^2}{R_\mathrm{v}^2}\cos\theta^2 + 1 - \frac{r_\mathrm{v}^2}{R_\mathrm{v}^2}} \,. \tag{24}$$

For the case $R_\mathrm{v} \leq r_\mathrm{v}$ we subtract one solution from the other to get the distance between the two crossings of the line of sight with the void boundaries. Therefore the dipole signal is proportional to

$$f = \sqrt{\frac{r_\mathrm{v}^2}{R_\mathrm{v}^2}\cos\theta^2 + 1 - \frac{r_\mathrm{v}^2}{R_\mathrm{v}^2}} \,, \tag{25}$$

where f is now the fraction of the dipole effect in the direction θ, meaning $d \propto f$. For the case of an observer on the edge of the void ($r_\mathrm{v} = R_\mathrm{v}$), this simplifies to a cosine and therefore behaves exactly like a kinetic dipole.

For the case $R_\mathrm{v} \geq r_\mathrm{v}$ one solution of (24) is negative. For an observer inside the void the fraction of the dipole effect depends on the difference of the length of the line of sight in the forward and backward direction. Thus, we need to add up the two solutions of (24) and obtain

$$f = \cos\theta \,. \tag{26}$$

Therefore an observer inside a void sees an effect for the dipole estimation which behaves like a cosine. So we can not distinguish this case from a kinetic dipole by its angular dependence.

In figure 6 we show the relation of f versus θ for different values of $r_\mathrm{v}/R_\mathrm{v}$. We see that this relation is steeper when the observer is outside the void ($r_\mathrm{v} > R_\mathrm{v}$). In future surveys, such an analysis can help to separate the kinetic dipole contribution from a structural component and also give an estimation of $r_\mathrm{v}/R_\mathrm{v}$.

The case investigated in this work is an observer living close to the edge of a void-like structure. This scenario cannot easily be distinguished from a pure kinetic dipole by this method, since both will behave like a cosine in angular dependence. Therefore the work of (Singal 2011) is not in conflict to the investigated scenario here.

5. Conclusion

We have been able to develop a model that can describe the influence of spherically symmetric local structures on linear dipole estimators. This model was tested and confirmed by computer simulations to a high level of accuracy. From this model we learn how the structure parameters (void size R_v, observer distance from the void centre r_v and void density contrast δ) influence the structure dipole amplitude.

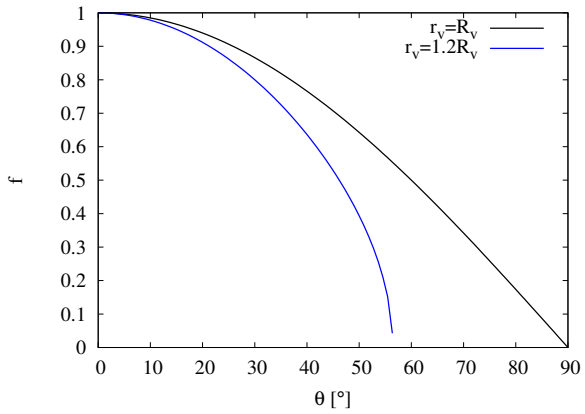

Fig. 6. Fraction of dipole effect f versus angle between dipole direction and line of sight θ for different ratios of the offset vector r_v to the void radius R_v.

Our analytical model requires a constant background density, which is a reasonable approximation at small redshifts. In order to include the effects of cosmic expansion and galaxy evolution, the dipole contribution for the realistic void model was estimated by means of simulations of the number counts of radio galaxies. Not included in this work are estimations of the dipole contribution from several galaxy clusters or other structures; because the dipole estimator is linear, these would just be a sum of terms similar to the ones calculated in this paper.

One might ask if a void as considered in this work would show up in the CMB. It is clear that the size of the effect will depend on the distance of the observer from the centre of the void. The CMB dipole will be maximally affected for an observer sitting at the edge of the void. There is no contribution to the CMB dipole if the observer sits in the centre and the effect would show up at much smaller angular scales if the observer were far away form the void. A CMB dipole would be induced by the integrated Sachs-Wolfe effect (or the Rees-Sciama effect if non-linear effects play a role) and thus the dynamics of the void profile would be important to determine its amplitude. Such structures have been studied previously, e.g. by Thompson & Vishniac (1987), Tomita (2000), Rakić et al. (2006), Inoue & Silk (2006), Maeda et al. (2011), Francis & Peacock (2010) and Rassat & Starck (2013). An order of magnitude estimate of the maximum possible effect (Panek 1992) gives

$$\Delta T/T \sim \delta^{3/2}\left(\frac{R_\mathrm{v}}{R_\mathrm{H}}\right)^3 \sim 2\times 10^{-4} \tag{27}$$

for the model considered here. This shows that the void-like structure considered in this paper would not be in tension with the observed CMB dipole, but might contribute to the CMB anomalies at small multipole moments. A detailed study of this topic is beyond the scope of this work.

For the void model of Keenan et al. (2013) for our local environment, we have run simulations which include a radio sky model from Wilman et al. (2008). We found that such a void already has a significant effect on the dipole estimation for surveys like the NVSS. The dipole amplitude measured by the linear estimator from Rubart & Schwarz (2013) of this void is expected to be $\tilde{d}_\mathrm{void} = 0.21 \pm 0.01 \times 10^{-2}$. The discrepancy between radio

and CMB dipole measurements can be relaxed by such a contribution, but the difference cannot be explained completely by the contribution from a single, realistic void. In forthcoming surveys, with lower flux density limits, the effect of local structure will become even more important.

Acknowledgements. MR and DJS acknowledge financial support from the Friedrich Ebert Stiftung and from the Deutsche Forschungsgemeinschaft, grant RTG 1620 "Models of Gravity". DB is supported by UK Science and Technology Facilities Council, grant ST/K00090X/1. Please contact the authors to request access to research materials discussed in this paper.

References

Alnes, H. & Amarzguioui, M. 2006, Phys.Rev., D74, 103520
Alnes, H., Amarzguioui, M., & Gron, O. 2006, Phys.Rev., D73, 083519
Bilicki, M. & Chodorowski, M. J. 2010, MNRAS, 406, 1358
Blake, C. & Wall, J. 2002, Nature, 416, 150
Celerier, M.-N. 2000, Astron.Astrophys., 353, 63
Condon, J. J., Cotton, W. D., Greisen, E. W., et al. 1998, AJ, 115, 1693
Crawford, F. 2009, ApJ, 692, 887
Francis, C. L. & Peacock, J. A. 2010, MNRAS, 406, 14
Gibelyou, C. & Huterer, D. 2012, MNRAS, 427, 1994
Hinshaw, G., Weiland, J. L., Hill, R. S., et al. 2009, ApJS, 180, 225
Inoue, K. T. & Silk, J. 2006, ApJ, 648, 23
Keenan, R. C., Barger, A. J., & Cowie, L. L. 2013, ApJ, 775, 62
Kogut, A., Lineweaver, C., Smoot, G. F., et al. 1993, ApJ, 419, 1
Kothari, R., Naskar, A., Tiwari, P., Nadkarni-Ghosh, S., & Jain, P. 2013, ArXiv e-prints 1307.1947
Maeda, K.-i., Sakai, N., & Triay, R. 2011, J. Cosmology Astropart. Phys., 8, 26
Panek, M. 1992, ApJ, 388, 225
Rakić, A., Räsänen, S., & Schwarz, D. J. 2006, MNRAS, 369, L27
Rassat, A. & Starck, J.-L. 2013, A&A, 557, L1
Rubart, M. & Schwarz, D. J. 2013, A&A, 555, A117
Singal, A. K. 2011, ApJ, 742, L23
Thompson, K. L. & Vishniac, E. T. 1987, ApJ, 313, 517
Tomita, K. 2000, ApJ, 529, 26
Whitbourn, J. R. & Shanks, T. 2014, MNRAS, 437, 2146
Wilman, R. J., Miller, L., Jarvis, M. J., et al. 2008, MNRAS, 388, 1335